Langmuir

Article

pubs.acs.org/Langmuir

Enantiospecific Adsorption of Amino Acids on Naturally Chiral Cu{3,1,17}$^{R\&S}$ Surfaces

Yongju Yun and Andrew J. Gellman*

Department of Chemical Engineering, Carnegie Mellon University, Pittsburgh, Pennsylvania 15213, United States

ABSTRACT: Gas-phase equilibrium adsorption of D- and L-serine (Ser) mixtures and D- and L-phenylalanine (Phe) mixtures has been studied on the naturally chiral Cu{3,1,17}$^{R\&S}$ surfaces. ^{13}C labeling of the L enantiomers (*L-Ser and *L-Phe) has enabled mass spectrometric enantiodiscrimination of the species desorbing from the surface following equilibrium adsorption. On the Cu{3,1,17}$^{R\&S}$ surfaces, both equilibrium adsorption and the thermal decomposition kinetics of the D and *L enantiomers exhibit diastereomerism. Following exposure of the surfaces to D/*L mixtures, the relative equilibrium coverages of the two enantiomers are equal to their relative partial pressures in the gas phase, $\theta_D/\theta_{*L} = P_D/P_{*L}$. This implies that adsorption is not measurably enantiospecific. The decomposition kinetics of Ser are enantiospecific whereas those of Phe are not. Comparison of these results with those for aspartic acid, alanine, and lysine suggests that enantiospecific adsorption on the naturally chiral Cu surfaces occurs for those amino acids that have side chains with functional groups that allow strong interactions with the surface. There is no apparent correlation between amino acids that exhibit enantiospecific adsorption and those that exhibit enantiospecific decomposition kinetics.

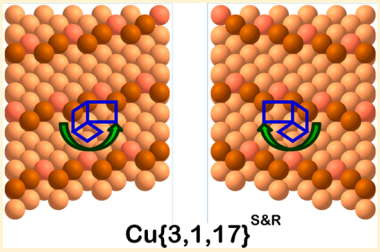

1. INTRODUCTION

In life on Earth, biomolecules such as peptides, proteins, DNA, RNA, and sugars are chiral and exist in only one enantiomeric form.[1,2] This homochiral biochemistry of living organisms has important implications for the synthesis of chiral bioactive compounds such as pharmaceuticals because the two enantiomers of a chiral bioactive molecule can have significantly different physiological impacts in the homochiral environment of the living organism into which they are ingested.[3,4] However, in the absence of a chiral environment, traditional chemical synthesis processes yield racemic (equimolar) mixtures of the two enantiomers of synthetic chiral compounds. As a result, enantioselective chemical processing in chiral media is an important subject of research in the pharmaceutical and agrochemical industries. The development of enantioselective chiral heterogeneous catalysts to produce enantiomerically pure compounds has attracted a great deal of attention over the past decade because heterogeneous catalysts have inherent advantages over homogeneous catalysts.[5−8] Among other things, heterogeneous catalysts are much more easily separated from their reaction products than are homogeneous catalysts. Given that enantioselective reactions can occur on chiral surfaces, developing a fundamental understanding of enantioselective surface chemistry is essential to the rational design and development of new enantioselective heterogeneous catalysts.

As model systems for the study of enantioselective catalytic processes, metal surfaces have been chirally modified by the irreversible adsorption of chiral organic molecules.[9−11] However, clean metal surfaces without modifiers can also be chiral. Although metals have achiral bulk crystal structures, intrinsically chiral metal surfaces can be generated by cleaving the bulk metal crystal along a low-symmetry direction and by exposing high Miller index planes with no mirror symmetry.[12,13] As an example, the two enantiomorphs of the naturally chiral Cu{3,1,17}$^{R\&S}$ surfaces used in this work are illustrated in Figure 1. The ideal structures of the surfaces have (100) terraces separated by kinked steps formed by (110) and (111)

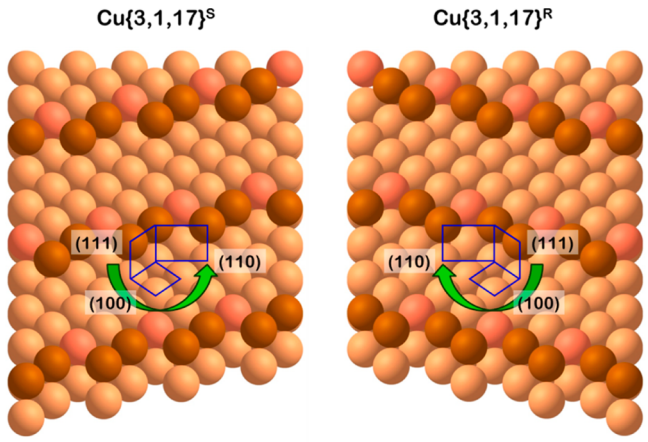

Figure 1. Ball model depiction of the ideal structures of the naturally chiral Cu{3,1,17}$^{R\&S}$ surfaces. The Cu{3,1,17}$^{R\&S}$ surfaces have kinked steps formed by (110) and (111) microfacets, separated by (100) terraces. The three microfacets forming each kink have opposite rotational orientation; therefore, the surfaces are nonsuperimposable mirror images of one another. The structures with clockwise and counterclockwise rotations, (111) → (100) → (110), are designated *R* and *S*, respectively.

Received: February 24, 2015
Revised: April 27, 2015
Published: May 1, 2015

DOI: 10.1021/acs.langmuir.5b00707
Langmuir 2015, 31, 6055−6063

microfacets. The mirror images of these structures are nonsuperimposable, and thus they are chiral. Scanning tunneling microscopy (STM) images of the Cu{643}^{R} surface show that the net chirality of the real structures of such high Miller index surfaces is preserved, in spite of the fact that they undergo thermal roughening.[14] Such naturally chiral metal surfaces are arguably the simplest model systems for the study of chiral surface chemistry, and they also have the potential to be more catalytically active and stable than achiral metal surfaces modified with chiral organic ligands.

The enantiospecific interactions of several chiral molecules with naturally chiral surfaces have been studied by various methods.[15−24] These enantiospecific interactions are the root cause of enantioselective catalysis and manifest themselves in enantiospecific differences in adsorption energetics and reaction kinetics. Hence, the detection of enantiospecificity in elementary surface reactions is a prerequisite for understanding the origin of enantioselectivity in catalysis and in other chemical processes mediated by chiral surfaces. The experimental detection of enantiospecific surface chemistry is challenging due to subtle differences in the interaction energies of one enantiomer of a chiral molecule with the two enantiomers of a chiral surface (or between the two enantiomers of a chiral molecule and one enantiomer of the chiral surface.) These energy differences are typically on the order of a few kJ/mol, but enantiospecific surface chemistry can be measured quantitatively using temperature-programmed desorption (TPD), X-ray photoelectron spectroscopy (XPS), and cyclic voltammetry.[18,22−25] Recently, we have developed a ^{13}C isotope labeling method for mass spectrometric enantiodiscrimination of amino acid enantiomers desorbing from or decomposing on surfaces. This has allowed direct measurement of the enantiospecificity of adsorption equilibrium constants from the relative coverages of amino acid enantiomers adsorbed under equilibrium conditions on chiral Cu{3,1,17}$^{R\&S}$ surfaces.[26,27] This approach relies on the fact that the L enantiomers of naturally occurring amino acids are available in ^{13}C-labeled form (herein denoted *L). Thus, equilibrium adsorption studies can be performed using gas-phase mixtures of D- and *L-amino acids, and their relative coverages on the surface can be measured by thermal decomposition to yield CO_2 and $^{13}CO_2$ whose yields can be quantified using mass spectrometry. On the Cu{3,1,17}^{R} surface, the ratio of enantiomer coverages, $\theta_{D/R}/\theta_{*L/R}$, at a given ratio of gas-phase pressures, P_D/P_{*L}, yields the ratio of the enantiospecific adsorption equilibrium constants, $K_{D/R}/K_{*L/R} = \theta_{D/R}P_{*L}/\theta_{*L/R}P_D$, and thereby the enantiospecific difference in their adsorption free energies, $\Delta\Delta G_{DL}$. On the Cu{3,1,17}$^{R\&S}$ surfaces, the results of these types of measurements are related by diastereomerism. By using various ratios of gas-phase pressures of the amino acid enantiomers, these experiments also allow discrimination between the adsorption of the amino acid mixtures in the form of racemate or conglomerate phases.[26]

One systematic approach to understanding enantiospecific adsorption on chiral surfaces is to study a homologous series of chiral probes on a naturally chiral surface. In previous work, we have studied the enantiospecific adsorption of several α-amino acids ($HO_2C-CH(NH_2)-R$) on the Cu{3,1,17}$^{R\&S}$ surfaces.[26−28] The enantiomers of aspartic acid (Asp, −R = $-CH_2CO_2H$) and lysine (Lys, −R = $-(CH_2)_4NH_2$) exhibit enantiospecific adsorption energies on the Cu{3,1,17}$^{R\&S}$ surfaces whereas alanine enantiomers (Ala, −R = $-CH_3$) do not. Herein, we report the enantiospecific adsorption energetics and decomposition kinetics of phenylalanine (Phe, −R = $-CH_2C_6H_5$) and serine (Ser, −R = $-CH_2OH$) on the naturally chiral Cu{3,1,17}$^{R\&S}$ surfaces using the ^{13}C-labeling methodology.

Prior studies of Ser on Cu single-crystal surfaces have examined its structure using STM, LEED, and NEXAFS.[29−31] On the achiral Cu(110) surface, Ser adsorbs anionically at 300 K via deprotonation of the carboxyl group. At a high coverage, θ = 0.25, the enantiomerically pure Ser overlayers are formed from dimers that are assembled into chiral, enantiomorphic overlayers. STM images show that racemic DL-Ser on Cu(110) forms overlayers containing small islands of homochiral dimers. Herein, we refer to racemic mixtures using the notation DL and to nonracemic mixture using the notation D/L. Temperature-programmed reaction (TPR) spectra of the enantiomerically pure D- or L-Ser showed CO_2 desorption from the Cu(110) surface at 470 K followed by a smaller CO_2 desorption feature at 520 K. The decomposition of racemic DL-Ser on Cu(110) yielded a low-temperature CO_2 desorption feature at 454 K and a smaller feature at 515 K. In spite of the fact that the DL-Ser forms small homochiral clusters on the Cu(110) surface, the presence of both enantiomers destabilizes the DL-Ser overlayer relative to the enantiomerically pure overlayers, with respect to decomposition. On the chiral Cu{531}$^{R\&S}$ surfaces, Ser adsorption was studied using NEXAFS and DFT.[29] The NEXAFS spectra were interpreted in terms of an anionic species with a deprotonated carboxylic acid group. At low coverages, the hydroxyl groups were also deprotonated, resulting in μ_4 geometry which DFT predicts to have a highly enantiospecific adsorption energy on the chiral Cu{531}$^{R\&S}$ surfaces, $\Delta\Delta E_{DL}$ = 50 kJ/mol. At high coverages, the hydroxyl group of adsorbed Ser is protonated, resulting in μ_3 geometry with much less enantiospecific adsorption energy, $\Delta\Delta E_{DL}$ = 3 kJ/mol. That work suggests that the enantiospecific adsorption of amino acids on a naturally chiral surface requires a side chain having strong interactions with the substrate.

The work reported herein studies Ser and Phe adsorption on the Cu{3,1,17}$^{R\&S}$ surfaces over a range of values of surface enantiomeric excess, $ee_s = (\theta_D - \theta_L)/(\theta_D + \theta_L)$. The relative equilibrium coverages of the two enantiomers of Phe and Ser in the presence of racemic gas-phase mixtures, $P_D = P_{*L}$, reveal no detectable enantiospecific adsorption. Although the lack of enantiospecific adsorption on the Cu{3,1,17}$^{R\&S}$ surfaces could be the result of an adsorbed racemate phase, equilibrium adsorption during exposure to nonracemic D/L mixtures in the gas phase shows that Phe and Ser both form conglomerate phases and that the adsorption energetics of the D and *L phases are not measurably enantiospecific, $\Delta\Delta G_{DL}$ = 0. In contrast, the decomposition kinetics of D- and *L-Ser on the Cu{3,1,17}$^{R\&S}$ surfaces do reveal enantiospecificity. However, the decomposition kinetics of Phe are not detectably enantiospecific. The combined results for Ala, Asp, Lys, Phe, and Ser adsorption and decomposition on Cu{3,1,17}$^{R\&S}$ surfaces reveal that the enantiospecificity of adsorption energetics is not correlated to the enantiospecificity of decomposition kinetics. More importantly, they suggest that bonding to the surface through a functional group in the side chain (−R) is one of the critical factors for inducing enantiospecific adsorption of the α-amino acids on the chiral Cu{3,1,17}$^{R\&S}$ surfaces.

DOI: 10.1021/acs.langmuir.5b00707
Langmuir 2015, 31, 6055−6063

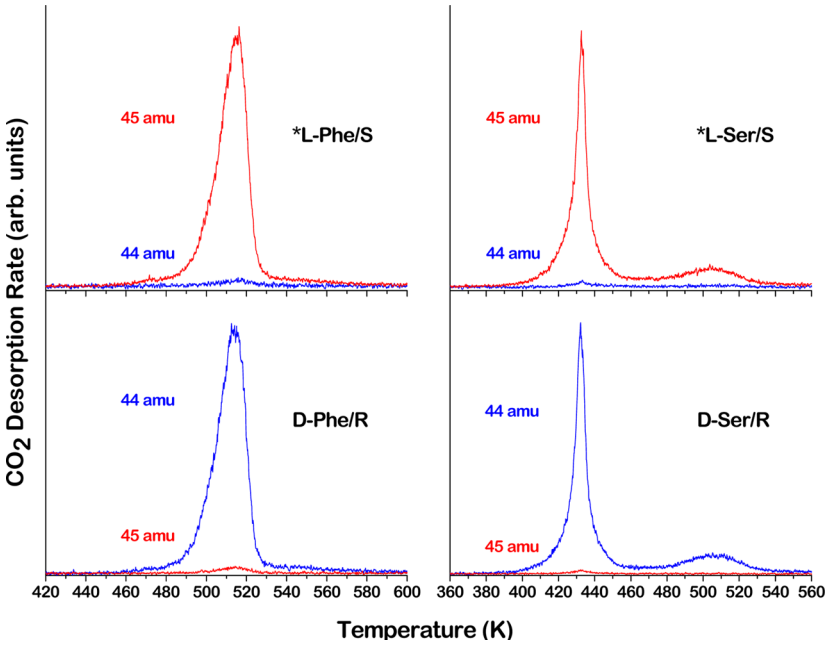

Figure 2. TPR spectra of enantiomerically pure Phe and Ser on Cu{3,1,17}$^{R\&S}$ at saturation coverage. The decomposition of D-Phe/Cu{3,1,17}^{R} and D-Ser/Cu{3,1,17}^{R} yields a TPRS signal at m/z = 44, almost exclusively. Equivalent chiral combinations of *L-Phe/Cu{3,1,17}^{S} and Ser/Cu{3,1,17}^{S} exhibit TPRS signals at m/z = 45, almost exclusively. The yields of CO_2 and $^{13}CO_2$ can be used to estimate the relative coverages of D and *L enantiomers of Phe and Ser.

2. EXPERIMENTAL SECTION

Enantiospecific adsorption of Phe and Ser on Cu{3,1,17}$^{R\&S}$ surfaces was studied in an ultrahigh vacuum (UHV), surface analysis chamber with a base pressure of 2×10^{-10} Torr. The chamber is equipped with an Ar^+ ion sputter gun to clean the Cu{3,1,17}$^{R\&S}$ surfaces, LEED optics to examine the ordering of clean surfaces, a homemade evaporator to deposit amino acids onto the Cu surfaces, and an Extrel mass spectrometer to detect chemical species in the gas phase and those desorbing from the surface.

The Cu{3,1,17}$^{R\&S}$ single-crystal sample (Monocrystals Company) was approximately 10 mm in diameter and 2 mm thick. The Cu single-crystal disk exposed the Cu{3,1,17}^{R} surface on one side and the Cu{3,1,17}^{S} surface on the other side. The temperature of the sample was varied over the range of 90−1000 K by resistive heating and liquid nitrogen cooling and was measured using a chromel−alumel thermocouple spot-welded to its edge. The temperature was controlled by a computer adjusting the heating current to give the desired temperature or heating rate. The Cu{3,1,17}$^{R\&S}$ sample was cleaned by repeated cycles of 1 keV Ar^+ ion sputtering while annealing at 850 K for 500 s. In the final step of the sputtering−annealing procedure, the sample was cooled at a controlled rate of −1 K/s at a pressure of $<1 \times 10^{-9}$ Torr in order to obtain a well-ordered surface structure. The long-range order of the clean Cu{3,1,17}$^{R\&S}$ surfaces was verified by LEED before the adsorption of each amino acid.

Isotopically labeled *L-Phe ($HO_2{}^{13}C-CH(NH_2)-CH_2C_6H_5$, 98% chemical purity, 99 atom %) and *L-Ser ($HO_2{}^{13}C-CH(NH_2)-CH_2OH$, 98% chemical purity, 99 atom %) were purchased from Cambridge Isotope Laboratories. Unlabeled D-Phe and D-Ser (99% chemical and optical purity) were purchased from Alfa Aesar. The amino acids were vapor deposited onto the Cu{3,1,17}$^{R\&S}$ surfaces by sublimation from a homemade evaporator with two glass vials, one for each enantiomer. The glass vials were wrapped with resistance heating wires, and the vial temperatures were measured by thermocouples bonded to their exteriors. The fluxes from each vial were controlled independently by heating the vials to different temperatures. The exposure times of the Cu{3,1,17}$^{R\&S}$ surfaces to the vapors were controlled by opening and closing a shutter placed in front of the glass vials. After exposure to Phe or Ser, the sample was positioned in front of the aperture to the mass spectrometer and then heated at 1 K/s to conduct temperature-programmed reaction spectroscopy (TPRS) of the adsorbed species. The relative coverages of D and *L enantiomers of Phe and Ser on the Cu{3,1,17}$^{R\&S}$ surfaces were determined by monitoring the signals of CO_2 (m/z = 44) and $^{13}CO_2$ (m/z = 45) with the mass spectrometer while heating the surfaces from 250 to 670 at 1 K/s and then integrating the signals across the temperature range in which the amino acid decomposed.

3. RESULTS

3.1. Enantiodiscrimination of Adsorbed D and *L Enantiomers by ^{13}C Labeling. The discrimination of enantiomers adsorbed on surfaces is critical to any study of enantioselective surface chemistry. Until recently, the only experiments capable of enantiodiscrimination of adsorbates were those using STM with sufficient resolution to distinguish enantiomer shapes on a surface.[32−35] For the study of amino acid mixtures on surfaces, we have developed a method for mass spectrometric enantiodiscrimination based on ^{13}C labeling of the L enantiomer.[26,27] Previous studies of amino acids on Cu surfaces showed that they adsorb on the surfaces in their anionic form and during thermal decomposition yield CO_2, presumably from their carboxylate groups.[26,36−40] Hence, mixtures of unlabeled D enantiomers and isotopically labeled *L enantiomers, in which the carboxylic acid group is ^{13}C-labeled, were used for the differentiation of the two enantiomers of Phe and Ser during their decomposition on the Cu{3,1,17}$^{R\&S}$ surfaces. To prevent multilayer formation during amino acid adsorption, the Cu{3,1,17}$^{R\&S}$ surfaces were held at 360 K and 350 K during exposure to Phe and Ser, respectively. Following saturation of the surface, the desorption signals at m/z = 44 and 45 arising from CO_2 and $^{13}CO_2$ evolution were monitored by mass spectrometry while heating the sample at 1 K/s.

TPR spectra of D and *L enantiomers of Phe and Ser on Cu{3,1,17}$^{R\&S}$ at saturation coverage are shown in Figure 2. As a result of isotopic labeling, *L-Phe decomposes, yielding a

DOI: 10.1021/acs.langmuir.5b00707
Langmuir 2015, 31, 6055−6063

product desorption signal at m/z = 45 that is far greater than the signal at m/z = 44. As expected, the signal at m/z = 44 is dominant during D-Phe decomposition. The same ratios of signals at m/z = 45 and 44 are seen in the TPR spectra of isotopically labeled *L-Ser and unlabeled D-Ser. These product desorption signals clearly show that the signals at m/z = 44 and 45 correspond to CO_2 and $^{13}CO_2$ desorption originating from the carboxylate groups of Phe and Ser. More importantly, the signals at m/z = 44 from the D enantiomers and at m/z = 45 from *L enantiomers can be used to quantify the relative coverages of the two enantiomers on the surface prior to thermal decomposition. It is also worth noting that the *L/*S* pair is diastereomerically equivalent to the D-/*R* pair. The fact that the isotopically labeled *L enantiomer/Cu{3,1,17}^{S} exhibits the same TPR spectra as the unlabeled D enantiomer/Cu{3,1,17}^{R} serves to demonstrate that there is no observable ^{13}C-isotope effect on the Phe or Ser decomposition kinetics and is consistent with control studies recently performed on the Cu(111) surface.[41]

3.2. Enantiospecific Decomposition of Phe and Ser on Cu{3,1,17}$^{R\&S}$. As mentioned, enantiospecific interactions of chiral molecules with naturally chiral surfaces manifest themselves in differences in reaction kinetics and adsorption energetics. In any measurement of an enantiospecific property such as the adsorption equilibrium constant for D or L adsorbates on *R* or *S* surfaces, the observation of a diastereomeric relationship, $K_{D/R} = K_{L/S} \neq K_{D/S} = K_{L/R}$, is necessary to demonstrate that the measurement is free of artifacts and sensitive only to the adsorbate and the surface chirality. Thus, the enantiospecific decomposition kinetics of Phe and Ser were examined by monitoring their CO_2 (m/z = 44) and $^{13}CO_2$ (m/z = 45) TPR spectra for all four combinations of D and L enantiomers on Cu{3,1,17}$^{R\&S}$ surfaces as shown in Figure 3. The decomposition kinetics of

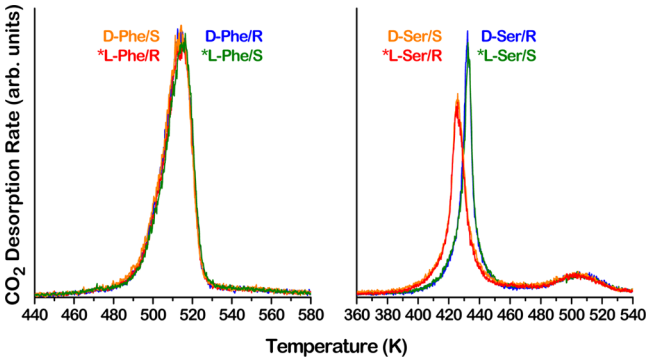

Figure 3. CO_2 and $^{13}CO_2$ TPR spectra from all four chiral combinations of D and *L enantiomers of Phe and Ser at saturation coverage on Cu{3,1,17}$^{R\&S}$. D- and *L-Phe/Cu{3,1,17}$^{R\&S}$ have identical TPR spectra, showing no enantiospecificity for the decomposition kinetics. The peak desorption temperature for D-Ser/Cu{3,1,17}^{R} (*L-Ser/Cu{3,1,17}^{S}) is ∼8 K higher than for D-Ser/Cu{3,1,17}^{S} (*L-Ser/Cu{3,1,17}^{R}), revealing an enantiospecific difference in decomposition kinetics on the chiral surfaces.

the Phe enantiomers on the Cu{3,1,17}$^{R\&S}$ surfaces are insensitive to the relative handedness of the adsorbate and the substrate, trivially meeting the criterion for the demonstration of diastereomerism.

The TPR spectra of Ser on the Cu{3,1,17}$^{R\&S}$ surfaces exhibit two separate peaks, a narrow CO_2 (or $^{13}CO_2$) peak at ∼430 K and a smaller peak at ∼505 K. Similar observations were reported for the decomposition of D- and L-Ser on Cu(110) and Cu{531}^{R};[40,42] however, the decomposition mechanism that gives rise to the two peaks in the TPR spectra of Ser on Cu surfaces is not completely understood. Although Phe exhibits identical TPR spectra for all four combinations of adsorbate/substrate enantiomers, Ser clearly shows a temperature difference between the TPR spectra for D-Ser/Cu{3,1,17}^{R} (*L-Ser/Cu{3,1,17}^{S}) and for D-Ser/Cu{3,1,17}^{S} (*L-Ser/Cu{3,1,17}^{R}). The narrow, low-temperature $^{13}CO_2$ desorption peak for *L-Ser occurs at 426 K on Cu{3,1,17}^{R} and at 434 K on Cu{3,1,17}^{S}. The narrow CO_2 desorption peaks of D-Ser exhibit the requisite diastereomerism. It is clear that the low-temperature peaks at 426 K are lower in intensity than those at 434 K. On initial inspection, it might appear that this is indicative of enantiospecific saturation coverages of D- and *L-Ser on Cu{3,1,17}$^{R\&S}$; however, the widths of the low-temperature peaks are also slightly greater than those of the high-temperature peaks, with the net effect being that the areas of the two are not significantly different and the measurement uncertainty in the peak areas being ±5%. No enantiospecificity was observed for the small TPRS peaks at 505 K. Either the species remaining adsorbed after the low-temperature Ser decomposition step are no longer chiral or, like Phe, they simply do not interact enantiospecifically with the Cu{3,1,17}$^{R\&S}$ surfaces.

One of the key features of our experimental methodology is the ability to expose the surfaces to gas-phase, binary mixtures of D and *L enantiomers with arbitrary but controlled composition. Although the relative coverages of enantiomers on the chiral surfaces are not necessarily the same as those in the gas phase, this allows us to investigate the influence of the surface enantiomeric excess, ee_s, of adsorbed Ser on its decomposition kinetics on the Cu{3,1,17}$^{R\&S}$ surfaces. The effect of ee_s was examined by varying the relative coverages of D- and *L-Ser on Cu{3,1,17}^{R} at saturation coverage and then monitoring TPR spectra during heating. The TPR spectra in Figure 4 from D-/*L-Ser mixtures on Cu{3,1,17}^{R} are the sum of the signals at m/z = 44 (D-Ser) and at m/z = 45 (*L-Ser). The individual peaks from the decomposition of the two enantiomers appear at almost the same temperature (see next paragraph) for each of the mixtures. The combined peak (CO_2

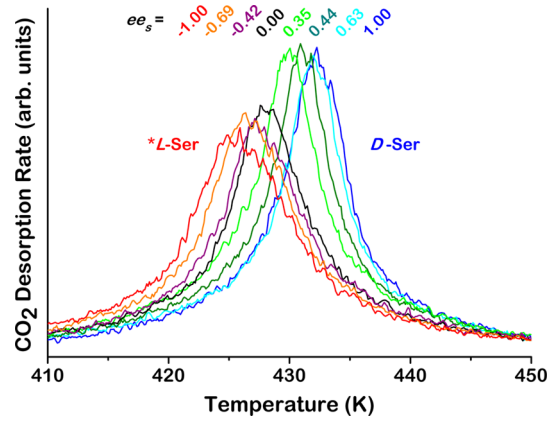

Figure 4. TPR spectra of binary mixtures of D- and *L-Ser on the Cu{3,1,17}^{R} surface at saturation coverage as a function of enantiomeric excess, ee_s, in the overlayer. The spectra were obtained by adding the signals at m/z = 44 and 45. As ee_s increases, the peak temperature shifts monotonically from enantiopure *L-Ser (red line) to enantiopure D-Ser (blue line).

DOI: 10.1021/acs.langmuir.5b00707
Langmuir 2015, 31, 6055−6063

and $^{13}CO_2$) from D-/*L-Ser shifts monotonically from the decomposition temperature of enantiopure *L-Ser (red line) to that of enantiopure D-Ser (blue line) with increasing ee_s of D-Ser in the overlayer. Note also that the leading edges of the decomposition peaks shift monotonically to increasing temperature with increasing ee_s. In the case of racemic D*L-Ser (black line), the combined peak appears midway between the desorption features of the enantiopure D- and *L-Ser, also exhibiting intermediate width and peak height.

For further analysis, the kinetics of racemic D*L-Ser decomposition on Cu{3,1,17}$^{R\&S}$ and the desorption signals from D-Ser (m/z = 44) and *L-Ser (m/z = 45) are represented in Figure 5. Although the difference in enantiospecificity is small, D-Ser starts to decompose at higher temperature than does *L-Ser on Cu{3,1,17}^{R} and vice versa on Cu{3,1,17}^{S}. This is consistent with the order in which decomposition occurs for the enantiomerically pure species on the Cu{3,1,17}$^{R\&S}$ surfaces; however, the temperature difference between enantiomers for the D*L-Ser is ∼1 K, much less than the 8 K difference observed for the pure enantiomers.

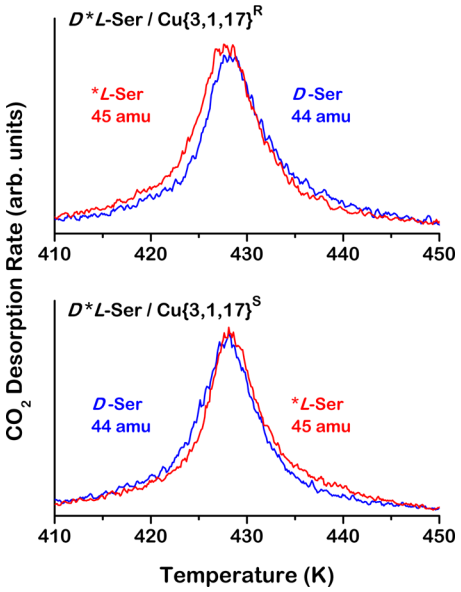

Figure 5. TPR spectra of racemic D*L-Ser on Cu{3,1,17}$^{R\&S}$ surfaces at saturation coverage. D-Ser starts to decompose at a higher temperature than does *L-Ser on Cu{3,1,17}^{R}. D-Ser starts to decompose at a lower temperature than does *L-Ser on Cu{3,1,17}^{S}. The ∼1 K enantiospecific difference in initial decomposition temperatures in D*L-Ser is much smaller than the 8 K difference in the decomposition temperature of the pure enantiomers (Figure 3).

3.3. Equilibrium Adsorption of Phe and Ser on Cu{3,1,17}$^{R\&S}$. Enantioselective equilibrium adsorption of Phe and Ser was studied by exposing Cu{3,1,17}$^{R\&S}$ surfaces to racemic and nonracemic mixtures in the gas phase for increasing periods of time to establish adsorption equilibria at saturation coverage. To establish equilibrium between gas-phase and adsorbed-phase species on the surface, rapid mutual displacement between D and *L enantiomers is required on the experimental time scale of ∼60 min. Previous studies of amino acid adsorption on Cu surfaces have shown that under a steady-state flux, displacement occurs once the surface is saturated with adsorbed species.[26,27] Thus, following saturation of the surface with Phe or Ser, the surface was held at 370 K (Ser) and 450 K (Phe) to allow rapid enantiomer displacement without any thermal decomposition during continued exposure. Control of the partial pressure ratio, P_D/P_{*L}, of the gas-phase mixtures was achieved by independently controlling the temperatures of the sublimation vials containing the pure D or *L enantiomers. As described above, following exposure of the surfaces to the gas-phase D/*L mixture for a given period of time, the ratio of D/*L enantiomer coverages, θ_D/θ_{*L}, was quantified using the CO_2 (m/z = 44) and $^{13}CO_2$ (m/z = 45) TPRS yields.

Figure 6 (left) shows the D-/*L-Ser coverage ratio, θ_D/θ_{*L}, on Cu{3,1,17}$^{R\&S}$ as a function of exposure time to D-/*L-Ser gas mixtures. The Cu{3,1,17}$^{R\&S}$ surfaces at 350 K were saturated with Ser after ∼15 min of exposure to the gas mixtures. During subsequent exposure of both Cu{3,1,17}^{R} (blue, ■) and Cu{3,1,17}^{S} (red, ★) at 370 K to racemic D*L-Ser, the value of θ_D/θ_{*L} remained unity for all exposure times, exhibiting no enantioselectivity. Enantioselective adsorption of one enantiomer would manifest itself by a deviation in θ_D/θ_{*L} from unity once the surface was saturated.[27] To be sure that θ_D/θ_{*L} = 1 is not simply due to low displacement rates, it is necessary to

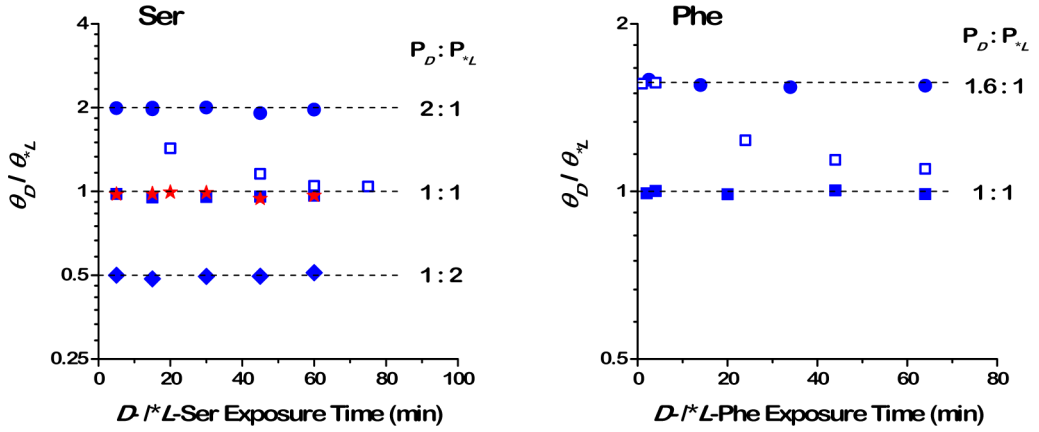

Figure 6. (Left panel) D-/*L-Ser coverage ratios, θ_D/θ_{*L}, on Cu{3,1,17}^{R} (blue symbols) and Cu{3,1,17}^{S} (red symbols) at 370 K as a function of exposure time to D-/*L-Ser gas mixtures with $P_D/P_{*L} = F_D/F_{*L} = {}^1/_2$, 1, and 2. The open square symbols were obtained using a partial pressure ratio of P_D/P_{*L} = 1 after starting with a surface coverage ratio of θ_D/θ_{*L} = 1.4. (Right panel) D-/*L-Phe coverage ratios, θ_D/θ_{*L}, on Cu{3,1,17}^{R} at 450 K as a function of exposure time to D-/*L-Phe gas mixtures with $P_D/P_{*L} = F_D/F_{*L}$ = 1 and 1.6. The open square symbols were obtained using a partial pressure ratio of P_D/P_{*L} = 1 after starting with a surface coverage ratio of θ_D/θ_{*L} = 1.6. At equilibrium, $\theta_D/\theta_{*L} = P_D/P_{*L}$ on both surface enantiomorphs.

DOI: 10.1021/acs.langmuir.5b00707
Langmuir 2015, 31, 6055−6063

perform a control experiment in which the surfaces are first saturated with a nonracemic mixture of D-/*L-Ser and then exposed to racemic D*L-Ser in the gas phase. The Cu{3,1,17}^{R} surface was first saturated with Ser having $\theta_D/\theta_{*_L} = 1.4$ and then exposed at 370 K to racemic gas-phase D*L-Ser. The continued exposure to racemic D*L-Ser resulted in a steady decrease in θ_D/θ_{*_L} from a value of 1.4 to reach unity after ~60 min (□). As with previous measurements using aspartic acid and alanine,[26,27] this result with Ser indicates that at 370 K the displacement rate between the gas phase and adsorbed phase is high enough to achieve adsorption equilibrium between enantiomers within the exposure time used.

Another adsorption scenario that would result in an equilibrium coverage ratio of $\theta_D/\theta_{*_L} = 1$ during exposure of Cu{3,1,17}$^{R\&S}$ to racemic D*L-Ser is the formation of an energetically stable racemate phase on the surface. Because the racemate phase has no net chirality, there would be no difference between its adsorption energetics on the Cu{3,1,17}$^{R\&S}$ surfaces. If the adsorbed racemate phase was significantly more stable than either of the enantiomerically pure conglomerate phases, then the value of θ_D/θ_{*_L} would be unity, independent of the partial pressure ratio of D- to *L-Ser. To determine whether exposure to nonracemic D-/*L-Ser mixtures leads to the formation of an adsorbed racemate phase, the equilibrium adsorption of D-/*L-Ser was examined by exposing the Cu{3,1,17}^{R} surface to gas-phase mixtures with $P_D/P_{*_L} = {}^1/_2$ and 2. The resulting coverage ratios (Figure 6 left, ● and ◆) show that $\theta_D/\theta_{*_L} = P_D/P_{*_L}$. These results are identical to those observed for alanine adsorption on Cu{3,1,17}$^{R\&S}$ and indicate that adsorbed Ser mixtures do not form a racemate phase nor do they adsorb enantiospecifically.[26]

In addition to the adsorption of D-/*L-Ser, we examined the equilibrium adsorption of D-/*L-Phe on Cu{3,1,17}^{R} at saturation coverage. Figure 6 (right panel) shows coverage ratios of D-/*L-Phe on Cu{3,1,17}^{R} at 450 K during exposure to a racemic mixture of gas-phase D*L-Phe (■) and a nonracemic mixture with $P_D/P_{*_L} = 1.6$ (●). As in the case of Ser, exposure of Cu{3,1,17}^{R} to racemic D*L-Phe simply results in the adsorption of a saturated Phe layer with $\theta_D/\theta_{*_L} = 1$. By starting with a Cu{3,1,17}^{R} surface prepared with an initial D-/*L-Phe coverage ratio of $\theta_D/\theta_{*_L} = 1.6$ and subsequently exposing it to racemic gas-phase D*L-Phe, the coverage ratio returns to $\theta_D/\theta_{*_L} \approx 1$ after ~60 min. This indicates that the displacement rate is sufficiently high at 450 K that a deviation from $\theta_D/\theta_{*_L} = 1$ would be observed if D- and *L-Phe adsorbed enantiospecifically. Starting with a Cu{3,1,17}^{R} surface prepared with an initial D-/*L-Phe coverage ratio of $\theta_D/\theta_{*_L} = 1.6$ and subsequently exposing it to gas-phase D-/*L-Phe with $P_D/P_{*_L} = 1.6$ results in adsorbed monolayers with $\theta_D/\theta_{*_L} = P_D/P_{*_L}$. Like Ser, Phe does not adsorb enantioselectively on Cu{3,1,17}$^{R\&S}$ surfaces; however, this lack of enantioselectivity is not the result of the formation of an adsorbed racemate phase.

4. DISCUSSION

4.1. Equilibrium Adsorption of D-/*L-Ser and D-/*L-Phe on Cu{3,1,17}$^{R\&S}$ Surfaces. As in the 3D crystallization of chiral mixtures, the adsorption of mixtures of D/L enantiomers onto surfaces can lead to three distinct types of phases: a racemate phase (DL), a conglomerate phase (2D domains of enantiomerically pure D or L adsorbates), or a random solid solution phase.[34,42−45] In the 3D crystallization of enantiomer mixtures, racemate phases are most common and random solid solutions are very uncommon. On a surface, the relative coverages of D and *L enantiomers, θ_D/θ_{*_L}, in equilibrium with gas-phase mixtures having various values of P_D/P_{*_L} provide insight into whether the adsorbed mixtures form racemate or conglomerate (or equivalently a random solution) phases. As shown in Figure 6, the exposure of Cu{3,1,17}$^{R\&S}$ surfaces to racemic D*L-Ser and D*L-Phe resulted in a coverage ratio of $\theta_D/\theta_{*_L} = 1$. One rationale for the adsorption of a racemic mixture, in spite of the fact that the surfaces are chiral and ought to adsorb one enantiomer preferentially, is that the enantiomers of Ser and Phe have no detectable enantiospecific difference in their adsorption free energies on the chiral Cu{3,1,17}$^{R\&S}$ surfaces, $\Delta\Delta G_{DL} \approx 0$. The other possibility is that adsorbed mixtures of D/*L enantiomers form racemate phases that are much more stable than the adsorbed conglomerate phases. Although the enantiomerically pure domains of the conglomerate phase could interact enantiospecifically with the chiral Cu{3,1,17}$^{R\&S}$ surfaces, the racemate domains could not. If the racemate phase were much more stable than the conglomerate phase, then the enantiomer ratio on the surface would be $\theta_D/\theta_{*_L} \approx 1$ for gas-phase mixtures with a wide range of enantiomeric excess (but obviously not those approaching $ee_g = (P_D - P_{*_L})/(P_D + P_{*_L}) = \pm 1$). The fact that exposing the Cu{3,1,17}$^{R\&S}$ surfaces to nonracemic mixtures of Ser or Phe resulted in $\theta_D/\theta_{*_L} = P_D/P_{*_L} \neq 1$ clearly shows that the formation of a very stable racemate phase can be ruled out. Hence, adsorbed D-/*L-Ser or D-/*L-Phe mixtures must form conglomerate phases on Cu{3,1,17}$^{R\&S}$ surfaces, but the adsorption free energies of their two enantiomers are not measurably enantiospecific, $\Delta\Delta G_{DL} = 0$. This is consistent with the results of prior DFT calculations of the adsorption energies of D- and L-Ser on the Cu{531}^{S} surface.[29] At high coverage, Ser has an intact hydroxyl group and is bonded to the surface in a μ_3 configuration through the deprotonated carboxylate group and the amine. D- and L-Ser have identical adsorption energies of 192 kJ/mol on the {110} facets of the Cu{531}^{S} surface, the sites of highest binding energy.

The TPR spectra of binary mixtures of D- and *L-Ser provide additional insight into the spatial extent of the enantiomerically pure domains formed during Ser adsorption on Cu{3,1,17}$^{R\&S}$. The TPR spectra obtained from enantiomerically pure D- and *L-Ser exhibit an enantiospecific difference of 8 K in the CO_2 desorption peak temperatures associated with the initial decomposition step. TPR spectra (Figure 4) of mixed monolayers of varying ee_s on the Cu{3,1,17}^{R} surface reveal that the CO_2 peak temperature shifts monotonically from 426 K for *L-Ser ($ee_s = -1$) to 434 K for D-Ser ($ee_s = 1$). Furthermore, using the $m/z = 44$ and 45 signals to distinguish the decomposition kinetics of D-Ser and *L-Ser in the racemic D*L-Ser monolayer shows that the two decompose almost concurrently (Figure 5). There is a barely detectable (~1 K) bias for the initial onset of *L-Ser decomposition on Cu{3,1,17}^{R} and D-Ser decomposition on Cu{3,1,17}^{S}. If adsorbed *L-Ser and D-Ser formed large homochiral domains on the Cu{3,1,17}$^{R\&S}$ surfaces, then one would expect that the decomposition kinetics observed in TPRS would reveal two resolved CO_2 and $^{13}CO_2$ peaks for the enantiospecific decomposition of the two Ser enantiomers. The data in Figures 4 and 5 are consistent with the formation of small homochiral clusters that are sufficiently interspersed that the decomposition of clusters of one enantiomer triggers the decomposition of the other enantiomer. This is consistent with observations of the decomposition of D-, L-, and DL-Ser on

DOI: 10.1021/acs.langmuir.5b00707
Langmuir 2015, 31, 6055−6063

Cu(110).[42] STM revealed that the adsorption of DL-Ser on Cu(110) results in the formation of small homochiral clusters, but TPRS reveals that the onset of DL-Ser decomposition occurs ~16 K lower than the decomposition of the enantiopure monolayers. In other words, the interspersion of domains of opposite handedness decreases the thermal stability of DL-Ser on Cu(110) relative to that of the pure enantiomers.

The mechanism of Ser decomposition on Cu{3,1,17}$^{R\&S}$ is not well understood. The TPR spectra shown in Figures 2 and 3 are very similar to those reported for Ser decomposition on Cu(110).[42] TPR spectra on Cu{3,1,17}$^{R\&S}$ obtained over a range of initial coverages show characteristics of an explosive decomposition mechanism. As the initial coverage increases, the peak CO_2 desorption temperature shifts to higher temperatures and the leading edges of the TPR spectra undercut one another with increasing coverage; the initial rate decreases with coverage. Furthermore, the TPRS peaks are very narrow, with the fwhm ≈ 7 K for D-Ser on Cu{3,1,17}^{R}. Similar observations are reported for Ser on Cu(110). Adsorbed acids such as tartaric acid and aspartic acid have been shown to undergo explosive decomposition on several Cu single-crystal surfaces.[10,15,27,34] The explosion mechanism is one in which a vacancy is needed to induce decomposition; however, the decomposition of one adsorbate leads to the formation of a second vacancy, which then leads to the decomposition of two more adsorbates and four vacancies, thereby leading to autocatalytic acceleration of the surface reaction. In this type of scenario, the decomposition of small homochiral clusters or islands of one enantiomer could trigger the decomposition of islands of the more stable enantiomer, as observed in Figure 4.

4.2. Origins of Amino Acid Enantiospecificity on Cu{3,1,17}$^{R\&S}$ Surfaces. The work reported herein brings to a total of five the number of α-amino acids whose enantiospecific adsorption has been studied on Cu{3,1,17}$^{R\&S}$ surfaces: Ser, Phe, Ala, Lys, and Asp.[26−28] These studies have included measurements of enantiospecific adsorption and enantiospecific decomposition kinetics. Table 1 summarizes the results of these observations. One interesting observation is that enantiospecific adsorption energetics are not a necessary condition for the observation of enantiospecific decomposition kinetics. As shown in Figures 3 and 6, D- and *L-Ser on Cu{3,1,17}$^{R\&S}$ exhibit readily observable enantiospecific decomposition kinetics but negligible difference in their adsorption energetics. In contrast, no enantiospecific difference in decomposition kinetics was observed for Asp and Lys on Cu{3,1,17}$^{R\&S}$, although they reveal enantiospecific adsorption energies of $\Delta\Delta G_{DL}$ = 3.2 ± 0.3 and 2.6 ± 0.3 kJ/mol, respectively.[27,28] Finally, neither the decomposition kinetics nor the adsorption energetics of the D and *L enantiomers of Ala and Phe on Cu{3,1,17}$^{R\&S}$ show enantiospecificity.[26]

Table 1. Enantiospecific Interactions of Amino Acids with the Cu{3,1,17}^{R} Surfaces

amino acid	adsorption $\Delta\Delta E_{DL}$ (kJ/mol)[a]	decomposition ΔT_{DL} (K)[b]	reference
alanine (Ala)	0[c]	0[d]	26
	1[e]		26
phenylalanine (Phe)	0[c]	0[d]	this work
serine (Ser)	0[c]	8[d]	this work
lysine (Lys)	−2.6 ± 0.3[f]	N/A[g]	28
aspartic (Asp)	−3.2 ± 0.3[c]	0[d]	27

[a]$\Delta\Delta E_{DL} = \Delta E^{ads}_{D/R} - \Delta E^{ads}_{L/R}$ where $\Delta E > 0$ represents the adsorption energies. [b]$\Delta T_{DL} = T_{D/R} - T_{L/R}$ where T represents the peak temperatures for amino acid decomposition. Note that the mechanism of amino acid decomposition on Cu is not well understood and may be sufficiently complex that the extraction of kinetic barriers directly from peak decomposition temperatures is unwarranted. [c]Determined from equilibrium adsorption measurements using ^{13}C labeling of the L-amino acid. [d]Measured during TPRS while heating at 1 K/s. [e]Predicted by DFT calculations. [f]Estimated from temperature-programmed desorption. Note that at high coverages lysine desorbs molecularly from Cu{3,1,17}$^{R\&S}$ surfaces. [g]A fraction of lysine decomposes on Cu{3,1,17}$^{R\&S}$ surfaces, but only at low coverages.

To our knowledge, STM images of these α-amino acids on the Cu(001) surface are the only additional available experimental data relevant to their enantiospecific adsorption energetics on Cu{3,1,17}$^{R\&S}$ surfaces. The adsorption of L-Ala, L-Phe, or L-Lys on Cu(001) leads to the formation of chiral {3,1,17} facets as a result of step faceting and bunching.[46−50] There are eight chiral {3,1,17} facets vicinal to the (001) pole, four of which are {3,1,17}^{R} with the remainder being {3,1,17}^{S}. A TPD study of D- and L-Lys desorption from Cu(001) and Cu{3,1,17}$^{R\&S}$ showed that the formation of chiral Cu{3,1,17} facets arises from higher adsorption energies of D- and L-Lys on Cu{3,1,17}$^{R\&S}$ surfaces than on Cu(001).[28] One interesting characteristic of the faceting induced by L-Lys adsorption on Cu(001) is the exclusive, homochiral creation of {3,1,17}^{R} facets.[48,51] TPD experiments revealed that the adsorption energy of L-Lys is higher on Cu{3,1,17}^{R} than on Cu{3,1,17}^{S}, demonstrating that the enantioselective faceting of Cu(001) results from the enantiospecific adsorption energies of L-Lys on the chiral Cu{3,1,17}$^{R\&S}$ surfaces. In contrast to L-Lys, the adsorption of glycine, an achiral α-amino acid, on Cu(001) results in the formation of both {3,1,17}^{R} and {3,1,17}^{S} facets. Given that neither glycine nor Cu(100) is chiral, this is not surprising. As in the case of glycine, the STM images of L-Ala and L-Phe on Cu(100) show that the surface reconstruction induced by their adsorption also leads to roughly equal numbers of {3,1,17}^{R} and {3,1,17}^{S} facets. This is consistent with our observation by equilibrium adsorption that L-Ala and L-Phe do not adsorb enantiospecifically on Cu{3,1,17}$^{R\&S}$, $\Delta G_{L/R} = \Delta G_{D/R}$, and therefore, $\Delta\Delta G_{DL} = 0$.[26] In the cases of L-Asp and L-Ser, no information relevant to enantiospecificity can be deduced from STM images because no faceting is observed during their adsorption on Cu(100).[31,52]

The cumulative set of measurements of the enantiospecific adsorption energetics of Ala, Asp, Lys, Phe, and Ser raises fundamental questions. Of these five, why is it that only Asp and Lys exhibit enantioselective adsorption on the Cu-{3,1,17}$^{R\&S}$, and what is its origin? A consideration of the possible influences of different side groups −R on the enantioselectivity of α-amino acids provides some insight. It is expected that these amino acids adsorb on the Cu surfaces in their anionic state via deprotonation of the carboxyl group ($^{-}O_2C-CH(NH_2)-R$) and interact with the surfaces through the two O atoms of the carboxylate group and the N atom of the amine.[38,39,48,53] They can then adopt μ_3, μ_4, or μ_5 conformations depending on whether the side group interacts directly with the surface. The amine and the two oxygen atoms of the deprotonated carboxyl group provide three points of interaction so that molecules such as Gly and Ala adsorb in the μ_3 configuration. Previous studies of D- and L-Ala adsorption on Cu{531}$^{R\&S}$ surfaces reported an enantiospecific difference in the local adsorption geometries of the two enantiomers arising

DOI: 10.1021/acs.langmuir.5b00707
Langmuir 2015, 31, 6055−6063

from the steric hindrance between a methyl group of Ala and the substrate.[17] DFT calculations predict an enantiospecific adsorption geometry of D- and L-Ala on the Cu{3,1,17}$^{R\&S}$ surfaces accompanied by an enantiospecific adsorption energy difference of $\Delta\Delta E_{DL}$ = 1 kJ/mol.[26] STM images of L-Phe on Cu(001) suggested that at saturation coverage the bulky phenyl ring is tilted away from the surface to minimize the steric interaction with the Cu surface atoms.[47] Finally, in the case of Ser on Cu{531}$^{R\&S}$, XPS shows that at high coverages the hydroxyl group is not deprotonated and DFT calculations predict $\Delta\Delta E_{DL}$ = 0 kJ/mol.[29] Collectively, these results suggest that Ala, Ser, and Phe adopt a μ_3 configuration on the surface and, consistent with our measurements, that this does not give rise to measurably enantiospecific adsorption energetics.

In contrast to Ala and Phe, Ser has a hydroxyl group in its side chain that can form an additional bond with a Cu substrate if it deprotonates. XPS shows that at low coverages of Ser on the Cu{531}$^{R\&S}$ surfaces, the hydroxyl group in the Ser side chain is deprotonated and presumably forms a strong interaction with the Cu substrate.[29] This μ_4 configuration of adsorbed Ser also bonds to the surface through the two O atoms of the deprotonated carboxyl group and through the nitrogen atom in the amine group. DFT predicts that the adsorption energies of the μ_4 configurations of D- and L-Ser on the Cu{531}$^{R\&S}$ surface differ by $\Delta\Delta E_{DL}$ = 50 kJ/mol, which is much more enantiospecific than the value of $\Delta\Delta E_{DL}$ = 0 kJ/mol predicted for the μ_3 configurations adopted by Ser at high coverage.

In the cases of Asp and Lys adsorption on Cu{3,1,17}$^{R\&S}$, their functional groups are involved in bonding to the surface. STM images of L-Lys (R− = $H_2N(CH_2)_4$−) on Cu(001) suggest that Lys is bound to the surface through both carboxylate O atoms and both amino N atoms, resulting in μ_4 geometry.[48] As noted earlier, Lys does exhibit enantiospecific adsorption energetics on the Cu{3,1,17}$^{R\&S}$ surfaces.[28] An XPS study of Asp on Cu(110) shows that it is adsorbed as the biaspartate species ($^-O_2CCH_2$−CH(NH_2)CO_2^-) at saturation coverage.[53] The fact that the O 1s XP spectrum shows a single peak suggests that Asp adopts a μ_5 configuration in which all four carboxylate O atoms and the amino N atom are bound to the surface. Both Lys and Asp, species bonded to Cu surfaces in μ_4 and μ_5 configurations, respectively, exhibit measurably enantiospecific adsorption energetics on the Cu{3,1,17}$^{R\&S}$ surfaces.[27,28]

Our experimental data for the enantioselectivity of Ala, Asp, Lys, Phe, and Ser adsorption on Cu{3,1,17}$^{R\&S}$ surfaces suggest that bonding between amino acid side groups and chiral substrates is an important factor in their exhibiting enantiospecific adsorption energetics on naturally chiral Cu surfaces. The same conclusion has been reached on the basis of DFT calculations of D- and L-Ser on Cu{531}^{S} in conformation with the hydroxyl group in its protonated and its deprotonated states.[29] Although we describe the configurations of the amino acids on these surfaces in terms of the numbers of atoms involved in the binding to the substrate (μ_3, μ_4, and μ_5), one could also think of these results in terms of a classical three-point interaction model in which the footprint at the α-C atom accounts for two interactions with the chiral surface and the R− side chain accounts for the third interaction in some amino acids but not in others.

5. CONCLUSIONS

Equilibrium adsorption of D-/L-Ser and D-/L-Phe mixtures on the chiral Cu{3,1,17}$^{R\&S}$ surfaces does not exhibit enantioselectivity, $ee_s = ee_g$. The decomposition kinetics of D- and L-Ser on Cu{3,1,17}$^{R\&S}$ exhibit detectable enantiospecificity whereas those of D- and L-Phe do not. Comparison of the collected data for the adsorption of amino acids (Ala, Ser, Phe, Asp, and Lys) on the Cu{3,1,17}$^{R\&S}$ surfaces suggested that enantiospecific adsorption requires an amino acid side group that can interact strongly with the surface. The observation of enantiospecific decomposition kinetics among these amino acids is not correlated to the observation of enantiospecific adsorption.

AUTHOR INFORMATION

Corresponding Author

*E-mail: gellman@cmu.edu.

Notes

The authors declare no competing financial interest.

ACKNOWLEDGMENTS

This work was supported by the U.S. Department of Energy under grant number DE-FG02-12ER16330.

REFERENCES

(1) Bonner, W. A. The Origin and Amplification of Biomolecular Chirality. *Origins Life Evol. Biospheres* **1991**, *21*, 59−111.
(2) Bada, J. L. Biomolecules - Origins of Homochirality. *Nature* **1995**, *374*, 594−595.
(3) Merino, I. M.; Gonzalez, E. B.; Sanzmedel, A. Liquid-Chromatographic Separation of Penicillamine Enantiomers Derivatized with Opa/2-Me on a Beta-Cyclodextrin Bonded Phase. *Mikrochim. Acta* **1992**, *107*, 73−80.
(4) Smith, S. W. Chiral Toxicology: It's the Same Thing···Only Different. *Toxicol. Sci.* **2009**, *110*, 4−30.
(5) Mallat, T.; Orglmeister, E.; Baiker, A. Asymmetric Catalysis at Chiral Metal Surfaces. *Chem. Rev.* **2007**, *107*, 4863−4890.
(6) Baiker, A. Progress in Asymmetric Heterogeneous Catalysis: Design of Novel Chirally Modified Platinum Metal Catalysts. *J. Mol. Catal., A* **1997**, *115*, 473−493.
(7) Lorenzo, M. O.; Baddeley, C. J.; Muryn, C.; Raval, R. Extended Surface Chirality from Supramolecular Assemblies of Adsorbed Chiral Molecules. *Nature* **2000**, *404*, 376−379.
(8) Baddeley, C. J. Fundamental Investigations of Enantioselective Heterogeneous Catalysis. *Top. Catal.* **2003**, *25*, 17−28.
(9) Barlow, S. M.; Raval, R. Complex Organic Molecules at Metal Surfaces: Bonding, Organisation and Chirality. *Surf. Sci. Rep.* **2003**, *50*, 201−341.
(10) Parschau, M.; Romer, S.; Ernst, K. H. Induction of Homochirality in Achiral Enantiomorphous Monolayers. *J. Am. Chem. Soc.* **2004**, *126*, 15398−15399.
(11) Zaera, F. Chiral Modification of Solid Surfaces: A Molecular View. *J. Phys. Chem. C* **2008**, *112*, 16196−16203.
(12) McFadden, C. F.; Cremer, P. S.; Gellman, A. J. Adsorption of Chiral Alcohols on "Chiral" Metal Surfaces. *Langmuir* **1996**, *12*, 2483−2487.
(13) Gellman, A. J. Chiral Surfaces: Accomplishments and Challenges. *ACS Nano* **2010**, *4*, 5−10.
(14) Baber, A. E.; Gellman, A. J.; Sholl, D. S.; Sykes, E. C. H. The Real Structure of Naturally Chiral Cu{643}. *J. Phys. Chem. C* **2008**, *112*, 11086−11089.
(15) Gellman, A. J.; Huang, Y.; Feng, X.; Pushkarev, V. V.; Holsclaw, B.; Mhatre, B. S. Superenantioselective Chiral Surface Explosions. *J. Am. Chem. Soc.* **2013**, *135*, 19208−19214.
(16) Horvath, J. D.; Baker, L.; Gellman, A. J. Enantiospecific Orientation of R-3-Methylcyclohexanone on the Chiral Cu(643)$^{R\&S}$ Surfaces. *J. Phys. Chem. C* **2008**, *112*, 7637−7643.

DOI: 10.1021/acs.langmuir.5b00707
Langmuir 2015, 31, 6055−6063

(17) Gladys, M. J.; Stevens, A. V.; Scott, N. R.; Jones, G.; Batchelor, D.; Held, G. Enantiospecific Adsorption of Alanine on the Chiral Cu{531} Surface. *J. Phys. Chem. C* **2007**, *111*, 8331−8336.
(18) Schillinger, R.; Šljivančanin, Ž.; Hammer, B.; Greber, T. Probing Enantioselectivity with X-ray Photoelectron Spectroscopy and Density Functional Theory. *Phys. Rev. Lett.* **2007**, *98*, 136102.
(19) Rampulla, D. M.; Francis, A. J.; Knight, K. S.; Gellman, A. J. Enantioselective Surface Chemistry of R-2-Bromobutane on $Cu(643)^{R\&S}$ and $Cu(531)^{R\&S}$. *J. Phys. Chem. B* **2006**, *110*, 10411−10420.
(20) Kuhnle, A.; Linderoth, T. R.; Besenbacher, F. Enantiospecific Adsorption of Cysteine at Chiral Kink Sites on Au(110)-(1 × 2). *J. Am. Chem. Soc.* **2006**, *128*, 1076−1077.
(21) Horvath, J. D.; Koritnik, A.; Kamakoti, P.; Sholl, D. S.; Gellman, A. J. Enantioselective Separation on a Naturally Chiral Surface. *J. Am. Chem. Soc.* **2004**, *126*, 14988−14994.
(22) Attard, G. A.; Ahmadi, A.; Feliu, J.; Rodes, A.; Herrero, E.; Blais, S.; Jerkiewicz, G. Temperature Effects in the Enantiomeric Electro-Oxidation of D- and L-Glucose on $Pt\{643\}^{S}$. *J. Phys. Chem. B* **1999**, *103*, 1381−1385.
(23) Horvath, J. D.; Gellman, A. J. Enantiospecific Desorption of Chiral Compounds from Chiral Cu(643) and Achiral Cu(111) Surfaces. *J. Am. Chem. Soc.* **2002**, *124*, 2384−2392.
(24) Horvath, J. D.; Gellman, A. J. Enantiospecific Desorption of R- and S-Propylene Oxide from a Chiral Cu(643) Surface. *J. Am. Chem. Soc.* **2001**, *123*, 7953−7954.
(25) Huang, Y.; Gellman, A. J. Enantiospecific Adsorption of (R)-3-Methylcyclohexanone on Naturally Chiral $Cu(531)^{R\&S}$ Surfaces. *Catal. Lett.* **2008**, *125*, 177−182.
(26) Yun, Y.; Wei, D.; Sholl, D. S.; Gellman, A. J. Equilibrium Adsorption of D- and L-Alanine Mixtures on Naturally Chiral $Cu\{3,1,17\}^{R\&S}$ Surfaces. *J. Phys. Chem. C* **2014**, *118*, 14957−14966.
(27) Yun, Y.; Gellman, A. J. Enantioselective Separation on Naturally Chiral Metal Surfaces: D-,L-Aspartic Acid on $Cu(3,1,17)^{R\&S}$ Surfaces. *Angew. Chem., Int. Ed.* **2013**, *52*, 3394−3397.
(28) Cheong, W. Y.; Gellman, A. J. Energetics of Chiral Imprinting of Cu(100) by Lysine. *J. Phys. Chem. C* **2011**, *115*, 1031−1035.
(29) Eralp, T.; Levins, A.; Shavorskiy, A.; Jenkins, S. J.; Held, G. The Importance of Attractive Three-Point Interaction in Enantioselective Surface Chemistry: Stereospecific Adsorption of Serine on the Intrinsically Chiral Cu{531} Surface. *J. Am. Chem. Soc.* **2012**, *134*, 9615−21.
(30) Eralp, T.; Shavorskiy, A.; Zheleva, Z. V.; Held, G.; Kalashnyk, N.; Ning, Y.; Linderoth, T. R. Global and Local Expression of Chirality in Serine on the Cu{110} Surface. *Langmuir* **2010**, *26*, 18841−18851.
(31) Iwai, H.; Emori, A.; Egawa, C. STM Study of L-Serine Adsorption on Cu(001). *Surf. Sci.* **2006**, *600*, 1670−1673.
(32) Bohringer, M.; Morgenstern, K.; Schneider, W. D.; Berndt, R. Separation of a Racemic Mixture of Two-Dimensional Molecular Clusters by Scanning Tunneling Microscopy. *Angew. Chem., Int. Ed.* **1999**, *38*, 821−823.
(33) Bohringer, M.; Schneider, W. D.; Berndt, R. Real Space Observation of a Chiral Phase Transition in a Two-Dimensional Organic Layer. *Angew. Chem., Int. Ed.* **2000**, *39*, 792.
(34) Romer, S.; Behzadi, B.; Fasel, R.; Ernst, K. H. Homochiral Conglomerates and Racemic Crystals in Two Dimensions: Tartaric Acid on Cu(110). *Chem.—Eur. J.* **2005**, *11*, 4149−4154.
(35) Seibel, J.; Zoppi, L.; Ernst, K. H. 2D Conglomerate Crystallization of Heptahelicene. *Chem. Commun.* **2014**, *50*, 8751−8753.
(36) Barlow, S. M.; Kitching, K. J.; Haq, S.; Richardson, N. V. A Study of Glycine Adsorption on a Cu{110} Surface Using Reflection Absorption Infrared Spectroscopy. *Surf. Sci.* **1998**, *401*, 322−335.
(37) Efstathiou, V.; Woodruff, D. P. Characterisation of the Interaction of Glycine with Cu(100) and Cu(111). *Surf. Sci.* **2003**, *531*, 304−318.
(38) Eralp, T.; Shavorskiy, A.; Zheleva, Z. V.; Dhanak, V. R.; Held, G. Hydrogen Bond-Induced Pair Formation of Glycine on the Chiral Cu{531} Surface. *Langmuir* **2010**, *26*, 10918−10923.
(39) Williams, J.; Haq, S.; Raval, R. The Bonding and Orientation of the Amino Acid L-Alanine on Cu{110} Determined by Rairs. *Surf. Sci.* **1996**, *368*, 303−309.
(40) Eralp, T.; Cornish, A.; Shavorskiy, A.; Held, G. The Study of Chiral Adsorption Systems Using Synchrotron-Based Structural and Spectroscopic Techniques: Stereospecific Adsorption of Serine on Au-Modified Chiral Cu{531} Surfaces. *Top. Catal.* **2011**, *54*, 1414−1428.
(41) Yun, Y.; Gellman, A. J. Adsorption-Induced Auto-Amplification of Enantiomeric Excess on an Achiral Surface. *Nat. Chem.* **2015**, DOI: 10.1038/nchem.2250.
(42) Eralp, T.; Shavorskiy, A.; Zheleva, Z. V.; Held, G.; Kalashnyk, N.; Ning, Y.; Linderoth, T. R. Global and Local Expression of Chirality in Serine on the Cu{110} Surface. *Langmuir* **2010**, *26*, 18841−51.
(43) Haq, S.; Massey, A.; Moslemzadeh, N.; Robin, A.; Barlow, S. M.; Raval, R. Racemic Versus Enantiopure Alanine on Cu(110): An Experimental Study. *Langmuir* **2007**, *23*, 10694−10700.
(44) Kuhnle, A.; Linderoth, T. R.; Hammer, B.; Besenbacher, F. Chiral Recognition in Dimerization of Adsorbed Cysteine Observed by Scanning Tunnelling Microscopy. *Nature* **2002**, *415*, 891−893.
(45) Santagata, N. M.; Lakhani, A. M.; Davis, B. F.; Luo, P. S.; Nardelli, M. B.; Pearl, T. P. Chiral Steering of Molecular Organization in the Limit of Weak Adsorbate-Substrate Interactions: Enantiopure and Racemic Tartaric Acid Domains on Ag(111). *J. Phys. Chem. C* **2010**, *114*, 8917−8925.
(46) Zhao, X. Y.; Zhao, R. G.; Yang, W. S. Adsorption of Alanine on Cu(001) Studied by Scanning Tunneling Microscopy. *Surf. Sci.* **1999**, *442*, L995−L1000.
(47) Wang, H.; Zhao, X. Y.; Zhao, R. G.; Yang, W. S. Adsorption of L-Phenylalanine on Cu(001). *Chin. Phys. Lett.* **2001**, *18*, 445−448.
(48) Zhao, X. Y.; Zhao, R. G.; Yang, W. S. Scanning Tunneling Microscopy Investigation of L-Lysine Adsorbed on Cu(001). *Langmuir* **2000**, *16*, 9812−9818.
(49) Zhao, X. Y.; Wang, H.; Zhao, R. G.; Yang, W. S. Self-Assembly of Amino Acids on the Cu(001) Surface. *Mater. Sci. Eng. C* **2001**, *16*, 41−50.
(50) Chen, Q.; Richardson, N. V. Surface Facetting Induced by Adsorbates. *Prog. Surf. Sci.* **2003**, *73*, 59−77.
(51) Zhao, X. Y. Fabricating Homochiral Facets on Cu(001) with L-Lysine. *J. Am. Chem. Soc.* **2000**, *122*, 12584−12585.
(52) Wang, H.; Zhao, X. Y.; Yang, W. S. Adsorption of Aspartic Acid on Cu(001) Studied by Scanning Tunneling Microscopy. *Acta Phys. Sin.* **2000**, *49*, 1316−1320.
(53) Mhatre, B. S. Super-Enantiospecific Autocatalytic Decomposition of Tartaric Acid and Aspartic Acid on Cu Surfaces. Ph.D. Thesis, Carnegie Mellon University: Pittsburgh, PA, 2013.

DOI: 10.1021/acs.langmuir.5b00707
Langmuir 2015, 31, 6055−6063